IEEE Access
Multidisciplinary | Rapid Review | Open Access Journal

Date of publication xxxx 00, 0000, date of current version xxxx 00, 0000.

Digital Object Identifier xxxx/ACCESS.xxxx.DOI

Demand-for graph and its state transition expression evaluating traffic congestion due to CAVs control

YUKARI MOCHIZUKI[1], (Not, IEEE Member), AND KENJI SAWADA[2], (Member, IEEE)

[1]Info-Powered Energy System Research Center, The University of Electoro-Communications; 1-5-1, Chofugaoka, Chofu city, Tokyo 182-8585, JAPAN (e-mail: ykr.mochizuki@uec.ac.jp)

[2]Info-Powered Energy System Research Center, The University of Electoro-Communications, 1-5-1, Chofugaoka, Chofu city, Tokyo 182-8585, JAPAN (e-mail: knj.sawada@uec.ac.jp)

Corresponding author: Yukari Mochizuki (e-mail: ykr.mochizuki@uec.ac.jp).

This paper is funded by JSPS KAKENHI Grant Number 23H01636, 23K03915,22H00519, 22H01509, and JP19H02158.

ABSTRACT Automated driving technologies are expected to reduce traffic congestion. Research studies have been conducted on the use of multi-agents as a method for analyzing and resolving traffic congestion involving a mixture of automated and manually driven vehicles using connected automated vehicles (CAVs). Existing methods that use multi-agent flow and density can analyze the occurrence of congestion and its mitigation, but cannot sufficiently characterize the starting point of congestion and the extent of its impact. By contrast, this study analyzes the interaction of communication and actions within agents, in addition to flow and density to identify the starting point of congestion and the extent of its influence. Specifically, we represent traffic flows consisting of manually and automatically driven vehicles as multi-agent systems consisting of cooperative and non-cooperative agents to evaluate the traffic congestion owing to altruistic lane changes by CAVs. Then, identify the starting point of congestion and the extent of its influence, a demand-for graph, which is a graph representation of the interaction of actions and communications among agents, is incorporated into the network search of an already existing asymmetric simple exclusion process. By deriving the state-transition equations of the adjacency matrix of the demand-for graph, this study clarifies the starting point, expansion, and resolution speed of congestion size due to altruistic lane changes. The results of this study enable the derivation of congestion occurrence and resolution conditions using the CAV control method for multiple traffic conditions.

INDEX TERMS Traffic congestion analysis, demand-for graph, connected automated vehicle (CAV)

I. INTRODUCTION

Multi-agent systems have a wide range of applications and, therefore, have been studied in various fields. Of particular note, is the mitigation of traffic congestion using the co-operative functions of agents, wichi, as a cross-disciplinary research topic, has been addressed in several research fields. For example, the use of connected automated vehicles (CAV) is expected to reduce traffic congestion [1]–[10]. However, although the facilitation of traffic flows composed solely of CAVs must also be studied, it dows not always apply to real scenarios, wherein traffic flows typically include cars that have not yet been replaced by CAVs. In addition, mal-functions, cyber-attacks, or incompatibilities among CAVs produced by different auto manufacturers [11] may prevent some CAVs from connecting to other. Traffic facilitation by CAVs may interfere with manually driven vehicles. Earlier studies [9], [10], [12]–[16] have considered control methods for automated vehicles operated in environments that include both automated and manually driven vehicles. A problem typically encountered in traffic facilitation using CAVs is the generation of speed shock waves caused by the stop and go motion of vehicles in traffic flow [1], [2], [6]–[10]. One crucial method for suppressing these speed shock waves is lane changing [6]–[8]. This study focuses on the generation and resolution of congestion in mixed flows composed of manually driven vehicles and CAVs as a result of coordinated lane changes by the CAVs.

When manually driven vehicles are present alongside CAVs in traffic, the formation and resolution of congestion must be considered. Congestion studies generally focus on

traffic flow under congested conditions. In Jamology, congestion is modeled as a state in which the flow rate of vehicles decreases as their density increases [17]–[22]. To analyze congestion in traffic networks, research studies have been conducted on asymmetric simple exclusion processes (ASEP) in multi-agent systems and ASEP network searches [17], [19], [21], [22]. When both automated and manually driven vehicles are present in traffic, the congestion caused by CAVs must be considered in addition to the conventional congestion caused by traffic concentration. In our previous study [23], we proposed a demand-for graph of congestion for evaluating the expansion and reduction in the scale of congestion owing to altruistic lane changes by CAVs under the cooperative control of agents.

Traffic flows depend on various factors such as road structure, traffic rules, and weather conditions, and thus, predicting and identifying the causes of traffic congestion is a problem that congestion studies have been trying to solve [24], [25]. Past studies [12]–[16] have analyzed the occurrence and mitigation of congestion from the viewpoint of traffic flow and density but have not sufficiently characterized the origin of congestion and the extent of its impact.

This study analyzes the interaction of communication and behavior within agents, in addition to flow and density, to identify the starting point and extent of the impact of congestion caused by agent control. To be able to evaluate traffic congestion due to altruistic lane change by CAVs, we first represent traffic flow involving manually and automatically driven vehicles as a network exploration of multi-agent systems consisting of cooperative and non-cooperative agents. Here, we derive the state transition equations of the adjacency matrix based on the communication and movement between agents according to the demand-for graphs of congestion proposed in our previous study [23]. Finally, we characterize the traffic congestion due to altruistic lane changes using these equations.

The first contribution of this study is (to the best of our knowledge) the first-ever visualization of the causal relationship between the occurrence and resolution of traffic congestion and the cooperative control of CAVs. The second contribution is the elucidation of the characteristics of traffic congestion due to altruistic lane changes by CAVs in traffic flows. The proposed congestion-analysis method based on the use of a demand-for graph allows for the effectiveness of cooperative control to be evaluated. Specifically, by clarifying the characteristics of the new congestion caused by introducing the cooperative function, the effectiveness of this function in easing the existing congestion and preventing new congestion can be assessed. This is also verified through numerical experiments.

The remainder of the paper is structured as follows. Section 2 describes the mathematical expressions and altruistic lane changes that constitute the problem setting of this study. Section 3 presents conventional congestion-analysis methods for the ASEP network search representation of traffic flow. Section 4 details the mathematical calculations for the altruistic lane change shown in Section 2 and the traffic-flow representation shown in Section 3. Section 5 presents the demand-for graphs corresponding to conventional congestion and congestion due to altruistic lane changes using the mathematical models shown in Sections 3 and 4, respectively. Section 6 provides a derivation of the state-transition equations corresponding to the adjacency matrix of the demand-for graphs shown in Section 5. Section 7 presents new proofs for the theorem derived in [23] using the state-transition equations of the adjacency matrix of the demand-for graphs shown in Section 6 and discussions on the characteristics of traffic congestion caused by altruistic lane changes. Finally, Section 8 provides a verification of the characteristics of the traffic congestion due to altruistic lane changes, previously described in Section 7, via numerical experiments and an evaluation of the changes in the flow rate of vehicles due to the introduction of CAVs.

II. PROBLEM SETTING

A. NOTATION

In this paper, the following notation is used frequently:

$$a = b, \tag{1}$$

$$a \leftarrow b, \tag{2}$$

$$a \equiv b, \tag{3}$$

$$a \supset b \equiv \neg a \vee b. \tag{4}$$

Equation (1) indicates the equivalence of the values a and b, whereas Equation (2) indicates the assignment of value b to the variable a. Equation (3) indicates that proposition a is a necessary and sufficient condition for proposition b, whereas Equation (4) states that it is a sufficient condition for proposition a to be true that proposition b to be true.

Herein, we use directed graphs to represent communication under cooperative behavior among agents and traffic congestion. We denote a directed graph comprising finite sets of nodes V and arcs E as $G = (V, E)$.

We denote the n-character unitary matrix as $\boldsymbol{I}_n$. Column vectors of order n where all elements are 0 and 1 are denoted as $\mathbf{0}_n$ and $\mathbf{1}_n$, respectively. The transpose of the matrix $\boldsymbol{M}$ is denoted as $\boldsymbol{M}^{\mathrm{T}}$.

B. LANE CHANGE AND VEHICLE GROUP FORMATION

First, we introduce findings from past research study [8] about CAVs changing lanes to facilitate traffic. In [8], a lane-change method for a group of automated vehicles with different speeds, to ensure the flow rate of the entire group of vehicles by ensuring the speed of each vehicle, was proposed. Each vehicle decides whether to move forward or change lanes based on its maximum speed, current speed, and target distance, and the maximum speed of the surrounding vehicles. When each vehicle determines that it cannot accelerate to the maximum speed simply by changing lanes on its own, it demands the vehicle in front to change lanes to facilitate traffic.

In this paper, the vehicle that demands the lane change and that which receives this demand are referred to as the current and front vehicles, respectively, as in [8]. The vehicle that receives a deceleration demand from the front vehicle is called the assistant vehicle. Under an altruistic lane change, the current, front, and assistant vehicles form a group of vehicles for cooperative control. In [8], to simplify the control, the vehicles that are already in the group reject any new lane change or deceleration requests. The front vehicle notifies the current and assistant vehicles that the lane has been changed, and the group of vehicles under altruistic lane change is released.

This study focuses on the deceleration required by the assistant vehicle for altruistic lane change and the temporary reduction in the speed of the vehicles behind the vehicle group, especially of that following the assistant vehicle. Therefore, we introduce a new concept, called an acceleration demand, for controlling CAVs to aid in evaluating the congestion due to altruistic lane changes and the deceleration required for changing lanes. When a vehicle pauses to avoid colliding with another vehicle belonging to a group, the former vehicle merges with the group and demands the latter vehicle to accelerate. Finally, we denote the vehicle that issued the acceleration demand as the follow vehicle. Therefore, the congestion due to the altruistic lane change is evaluated as a decrease in the speed and an increase in the density of the follow vehicle. In the following section, we refer to traffic congestion due to altruistic lane changes and their demand as altruistic congestion.

An example of an altruistic lane change and the formation of a group of vehicles for changing lanes by five CAVs is shown in Fig. 1, $\mathscr{A}_i \in \{\mathscr{A}_1, \mathscr{A}_2, \mathscr{A}_3, \mathscr{A}_4, \mathscr{A}_5\}$ denotes each CAV. The following two scenarios, shown in Fig. 1, are assumed: (1) the front of $\mathscr{A}_1$ is blocked by three vehicles ($\mathscr{A}_2$, $\mathscr{A}_3$, and $\mathscr{A}_4$), the maximum speeds of which are lower than that of $\mathscr{A}_1$; and (2) the speeds of $\mathscr{A}_2$, $\mathscr{A}_3$, and $\mathscr{A}_4$ are equal.

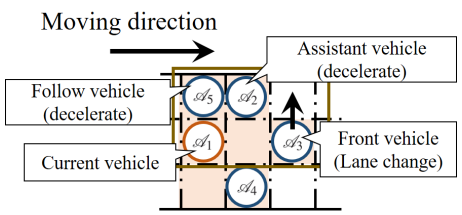

FIGURE 1: Altruistic lane change

If $\mathscr{A}_1$ attempts to move to any of the three lanes, it will be blocked by other vehicles and will be unable to reach its maximum speed. Then, $\mathscr{A}_1$ will demand a lane change from $\mathscr{A}_3$, which is located in front of $\mathscr{A}_1$ in the same lane as that of the current vehicle. Subsequently, $\mathscr{A}_3$ will be set as the front vehicle, but will be blocked from changing lanes by two vehicles, $\mathscr{A}_2$ and $\mathscr{A}_4$, occupying the lane and moving at almost equal speeds. Next, $\mathscr{A}_3$ will demand that $\mathscr{A}_2$ decelerate to maintain the distance required for the lane change. Therefore, $\mathscr{A}_2$ will be set as the assistant vehicle, and $\mathscr{A}_3$ will continue to move forward at the current speed until $\mathscr{A}_3$ can change lanes. At this point, $\mathscr{A}_5$ will decelerate to avoid collision with $\mathscr{A}_2$. After successfully changing its lane, $\mathscr{A}_3$ will notify $\mathscr{A}_1$ and $\mathscr{A}_2$ that it has completed its lane change. After receiving the notification, $\mathscr{A}_2$ will accelerate to the maximum speed to maintain vehicle speed. Consequently, $\mathscr{A}_1$ will be able to accelerate to its maximum speed owing to $\mathscr{A}_3$ changing lanes. The vehicle group includes a maximum of one each of the current, front, and assistant vehicles.

C. DEMANDS FOR ALTRUISTIC LANE CHANGE

In this study, we evaluate the relationship between lane change, deceleration, and acceleration demands associated with altruistic lane changes and the size of traffic congestion. In this subsection, we present the lane change, deceleration, and acceleration demands associated with the altruistic lane change of CAVs $\{\mathscr{A}_1, \mathscr{A}_2, \cdots, \mathscr{A}_I\}$. In the following, we denote the i-th vehicle among the CAVs as $\mathscr{A}_i$ ($i \in \mathscr{I} := \{1, 2, \cdots, I\}$). The value of i is considered to be the ID of the vehicle.

To increase their speed, vehicles have to request lane changes from those in front of them. The identification (ID) of the vehicle from which $\mathscr{A}_i$ demands a lane change at time t is denoted by $r_c(t,i) \in (\{0\} \cup \mathscr{I})$. If $\mathscr{A}_i$ does not request a lane change from another vehicle at time t, then $r_c(t,i) = 0$. Meanwhile, the ID of the vehicle that $\mathscr{A}_i$ demands to decelerate at time t is denoted by $r_d(t,i) \in (\{0\} \cup \mathscr{I})$. If $\mathscr{A}_i$ does not demand the declaration of other vehicles at time t, then $r_d(t,i) = 0$. Similarly, the ID of the vehicle that $\mathscr{A}_i$ demands to accelerate at time t is denoted by $r_a(t,i) \in (\{0\} \cup \mathscr{I})$. If $\mathscr{A}_i$ does not demand the acceleration of another vehicle at time t, then $r_a(t,i) = 0$. The ID of the vehicle that $\mathscr{A}_i$ demands to change lanes, decelerate, or accelerate at time t is denoted by $r(t,i) \in (\{0\} \cup \mathscr{I})$. If $\mathscr{A}_i$ does not demand that another vehicle to change lanes, decelerate, or accelerate at time t, then $r(t,i) = 0$. In this case, $r_c(t,i)$, $r_d(t,i)$, and $r_a(t,i)$ satisfy

$$\begin{aligned} &\neg\left(r_c(t,i) > 0\right) \vee \left(r(t,i) = r_c(t,i)\right), \\ &\neg\left(r_d(t,i) > 0\right) \vee \left(r(t,i) = r_d(t,i)\right), \\ &\neg\left(r_a(t,i) > 0\right) \vee \left(r(t,i) = r_a(t,i)\right). \end{aligned} \tag{5}$$

Equation (5) indicates that at time t, the maximum number of demands that $\mathscr{A}_i$ can set is 1. Consequently, $r(t,i)$ in terms of $r_c(t,i)$, $r_d(t,i)$, and $r_a(t,i)$ satisfies

$$r(t,i) = r_c(t,i) + r_d(t,i) + r_a(t,i). \tag{6}$$

III. FORMULATION OF MULTI-LANE ASEP SEARCH

In this study, we represent the single-road driving of a CAV, which can travel along a straight path, change lanes, and change speeds, as a multi-lane ASEP search on a multi-agent system. Based on this multi-lane ASEP search representation, congestion is then formulated as a decrease in the flow rate owing to an increase in the vehicle density.

Hereafter, for simplicity, the terms agent and vehicle will be used synonymously, unless otherwise specified.

A. ASEP

An ASEP consists of Y cells, including start and end cells. In an ASEP, the cells are arranged in a one-dimensional grid. Agents move from the start cell of the ASEP to the end cell. If the next cell is not occupied by other agents at time t, then every agent moves to the next cell with probability p at time $t+1$. The flow quantity of an agent in an ASEP depends on the density ρ $(0<\rho<1)$ of the agents in the ASEP. When ρ is greater or less than $1/2$, the flow quantity decreases or increases, respectively, in proportion to the increase in ρ.

An example ASEP of length Y is shown in Fig. 2. An agent in the ASEP moves from the start cell to the end of the ASEP, one plot at a time, with a certain probability. Agents can move only to the cells wherein no other agent is present. In Fig. 2, v_1 is called as the start cell of the ASEP, and if no agent is present in v_1, an agent will appear in v_1 with a certain probability. On the other hand, v_Y in Fig. 2 is called as the end cell of the ASEP. If an agent is present, it will disappear with a certain probability.

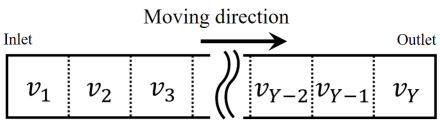

FIGURE 2: Example ASEP

The ASEP search system, i.e., the search for multi-lane ASEP $\mathscr{N}$ by I agents, is decentralized and involves a group of agents or vehicles capable of movement, speed change, and communication. In addition, each agent can altruistically change lanes and form vehicle groups, as will be demonstrated in Section 4. In this subsection, we mathematically model the movement of the agents in an ASEP.

The agent has self-position identification and surrounding-agent detection functions. For these functions, we define the binary variable $\varepsilon(t,i,v)\in\{0,1\}$, which indicates if $\mathscr{A}_i$ is in cell v at time t. If $\mathscr{A}_i$ is present in cell $v\in N$ at time t, then $\varepsilon(t,i,v)$ is 1. Otherwise, $\varepsilon(t,i,v)$ is 0. On the other hand, the position of $\mathscr{A}_i$ at time t is denoted as $\varepsilon_{\mathscr{A}}(t,i)\in N$. If no $\mathscr{A}_i$ is present at time t, then $\varepsilon_{\mathscr{A}}(t,i)$ is 0. Meanwhile, the ID of the agent present in cell $v\in N$ at time t is $\varepsilon_{\mathscr{N}}(t,v)\in(\{0\}\cup\mathscr{I})$. If no agent is present in cell v, $\varepsilon_{\mathscr{N}}(t,v)$ is 0. In this study, based on proposed method, we use $\varepsilon_{\mathscr{N}}(t,v)$ for the congestion analysis based on density and flow rate and $\varepsilon_{\mathscr{A}}(t,i)$ for the congestion evaluation based on agent motion interference. In this case, $\varepsilon_{\mathscr{N}}(t,v)$ satisfies the following conditions for $\varepsilon(t,i,v)$:

$$(\varepsilon_{\mathscr{N}}(t,v)=i)\ \equiv\ (\varepsilon(t,i,v)=1), \tag{7}$$

$$(\varepsilon_{\mathscr{N}}(t,v)=0)\equiv(\varepsilon(t,i,v)=0,\ \forall\, i\in\mathscr{I}). \tag{8}$$

The movement of $\mathscr{A}_i$ to v at time t is denoted as $\delta(t,i,v)\in\{0,1\}$. If $\mathscr{A}_i$ moves to v at time t, then $\delta(t,i,v)$ will be 1. Otherwise, $\delta(t,i,v)$ will be 0. The destination cell of $\mathscr{A}_i$ at time t is denoted as $\delta_{\mathscr{A}}(t,i)\in\mathscr{N}$, which satisfies the following conditions for $\delta(t,i,v)$:

$$(\delta_{\mathscr{A}}(t,i)=v)\equiv(\delta(t,i,v)=1). \tag{9}$$

Additionally, the target destination cell of $\mathscr{A}_i$ at time t is represented by $\hat{\delta}_{\mathscr{A}}(t,i)\in\mathscr{N}$. The agent either moves to the target destination cell or pauses to avoid a collision. Then, $\delta_{\mathscr{A}}(t,i)$ satisfies the following conditions for $\hat{\delta}_{\mathscr{A}}(t,i)\in\mathscr{N}$ and $\varepsilon_{\mathscr{A}}(t,i)$:

$$\begin{aligned}&\neg(\delta_{\mathscr{A}}(t,i)=v)\\ &\vee\left(\left(\hat{\delta}_{\mathscr{A}}(t,i)=v\right)\vee(\varepsilon_{\mathscr{A}}(t,i)=v)\right)\end{aligned}. \tag{10}$$

In this subsection, we denote the x-th compartment of the ASEP as v_x. Considering the distance traveled by the agent, $\delta_{\mathscr{A}}(t,i)$ satisfies

$$\neg(\delta_{\mathscr{A}}(t,i)=v_x)\vee(\varepsilon_{\mathscr{A}}(t,i)\in\{v_{x-1},v_x\}). \tag{11}$$

For $\delta_{\mathscr{A}}(t,i)$, $v=\hat{\delta}_{\mathscr{A}}$(t,i), and $\varepsilon(t,i,v)$, the conditions for pausing to avoid collision are as follows:

$$\neg\left(\sum_{j\in(\mathscr{I}\setminus\{i\}}\varepsilon(t,j,v)=1\right)\vee(\delta_{\mathscr{A}}(t,i)=\varepsilon_{\mathscr{A}}(t,i)) \tag{12}$$

When the left-hand side of (12) is satisfied, the vehicle pauses to avoid a collision.

In this study, the speed of an agent is expressed as a movement probability. The agent has two speed parameters, namely, the current and maximum speeds. The current speed of $\mathscr{A}_i$ at time t is denoted as $p(t,i)(0\le p(t,i)\le 1)$, whereas the maximum value of $p(t,i)$ is denoted as $p_{\max}(i)(0\le p_{\max}(i)\le 1)$, where $p_{\max}(i)$ denotes the maximum speed of $\mathscr{A}_i$. This study does not consider transient speeds in defining the accelerations and decelerations of the agents.

To be able to determine the behavior of $\mathscr{A}_i$, we express the congestion due to the overcrowding of agents as follows:

$$\varepsilon_{\mathscr{N}}\left(t,\hat{\delta}_{\mathscr{A}}(t,i)\right)\neq 0. \tag{13}$$

B. MULTI-LANE ASEP

A multi-lane ASEP is an ASEP network in which multiple ASEPs of equal lengths are connected in parallel. The search target is a multi-lane ASEP $N:=\mathscr{L}_1\cup\mathscr{L}_2\cup\cdots\cup\mathscr{L}_X$ with number of lanes X and length Y, where $\mathscr{L}_x:=\{v_1^x,v_2^x,\cdots,v_Y^x\}\,(1\le x\le X)$ represents the ASEP located in the x-th lane of N, and $v_y^x\in\mathscr{L}_x$ represents the y-th compartment of ASEP $\mathscr{L}_x$.

A multi-lane ASEP with number of lanes 3 and length 8 is shown in Fig. 3. An agent on the multi-lane ASEP can move to the previous cell and the adjacent ASEP. Fore example, the agent located at v_4^2 in Fig. 3 changes lanes to v_4^1 or v_4^3.

In this subsection, we extend the mathematical model of the movement of the agents to be able to accommodate multi-lane ASEP search.

During a multi-lane ASEP search, agents can change lanes to adjacent lanes in addition to moving forward. Therefore,

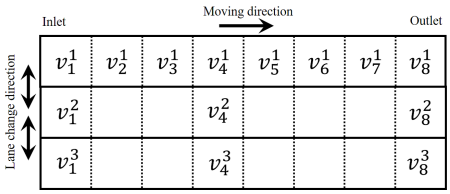

FIGURE 3: Multi-lane ASEP

the constraint equation (11) for the movement range of the agent is extended as follows:

$$\neg\left(\hat{\delta}_{\mathscr{A}}(t,i)=v_y^x\right)\vee\left(\varepsilon_{\mathscr{A}}(t,i)\in\{v_y^{x-1},v_{y-1}^x,v_y^x,v_y^{x+1}\}\right). \tag{14}$$

This study considers a straight-line priority rule to prevent collisions between agents. This rule restricts the movements of agents in the destination cell and of those in the adjacent cells behind the destination cell when changing lanes. Therefore, we extend the pausing condition for avoiding collisions as follows:

$$\begin{aligned}&\neg\left(\textstyle\sum_{j\in(\mathscr{I}\setminus\{i\})}\varepsilon\left(t,j,v_y^x\right)+\varepsilon\left(t,j,v_{y-1}^x\right)=1\right)\\&\vee\left(\delta_{\mathscr{A}}(t,i)=\varepsilon_{\mathscr{A}}(t,i)\right),\\&v_y^x=\hat{\delta}_{\mathscr{A}}(t,i).\end{aligned} \tag{15}$$

In [17]–[22], congestion was evaluated using the relationship between the densities of the agents, which are indicated by $\varepsilon(t,j,v)$, and the flow rate, which is derived from $\delta(t,i,v)$.

In this study, we clarify the relationship between the demand for altruistic lane change and the flow rate using the demand-for graphs presented in Section 5.

IV. CONTROL ALGORITHMS FOR CAVS

In this section, we extend the algorithms used for vehicle group formation and lane changes by the CAVs involved in the multi-lane ASEP search. Additionally, we present a mathematical model for setting the lane change, deceleration, and acceleration requirements of the vehicle.

When a vehicle receives a demand for lane change, deceleration, or acceleration from another vehicle, it forms a vehicle group with the demanding vehicle. The inclusion of $\mathscr{A}_i$ in the vehicle group at time t is denoted by $\xi(t,i)\in\{0,1\}$. At time t, if $\mathscr{A}_i$ is included in the vehicle group, then $\xi(t,i)=1$. We denote the notification of the separation of the vehicle groups containing $\mathscr{A}_i$ at time t,i as $g_c(t,i)\in\{0,1\}$. If $\mathscr{A}_i$ separates from the vehicle group at time t, then $g_c(t,i)=1$.

First, the vehicle determines whether a lane change must be demanded. For each lane, $\mathscr{A}_i$ determines the target distance $d\in\{1,2,...,\infty\}$ to be maintained and whether it can accelerate to $p_{\max}(i)$ within the target distance d. Then, $\mathscr{A}_i$ determines whether acceleration is possible in lane x' according to the speeds of the other vehicles within the target distance and its position $v_y^x=\varepsilon(t,i)$ using Algorithm 1.

Using Algorithm 2, $\mathscr{A}_i$ determines whether it is possible to accelerate to the maximum speed by changing lanes, based on whether acceleration is possible in each lane. If $\mathscr{A}_i$ determines that acceleration is impossible after a lane change, it sends a lane-change demand to the vehicle immediately in front of it in the same lane. In this case, the ID of the vehicle that receives the demand is set to $r_c(t,i)$. If the target vehicle already belongs to a vehicle group, then the lane-change demand is rejected. Then, for $\xi(t,i)$, $r_c(t,i)$ satisfies

$$\begin{aligned}&\neg\left((r_c(t,i)\neq r_c(t-1,i))\wedge(r_c(t,i)\neq 0)\right)\\&\vee\left(\xi\left(t,r_c(t,i)\right)=0\right)\end{aligned}. \tag{16}$$

In the case of $r_c(t,i)\neq 0$, $\mathscr{A}_i$ is the current vehicle and $\mathscr{A}_{r_c(t,i)}$ is the front vehicle that merges into the vehicle group.

Algorithm 1 VehicleDetectionForSingleLane(x'): Acceleration availability at $\mathscr{L}_{x'}$

```
Set x and y from v_y^x = ε_A(t,i);
if (|x' − x|) > d then
    return false;
else
    for l ← 1; l < d − |x' − x|; l++ do
        if (y + l ≤ Y) then
            if ( p_A(t, ε_M(t, v_{y+l}^{x'})) < p_max(t,i) ) then
                return false;
            end if
        end if
    end for
    return true;
end if
```

Algorithm 2 VehicleDetectionForMultileLane(): Acceleration on its own or not

```
Set x from v_y^x = ε_A(t,i);
if Function1(x)=true then
    return true;
end if
for (m ← 1; m < d; m++) do
    if VehicleDetectionForSingleLane(x + m)=true then
        return true;
    end if
    if VehicleDetectionForSingleLane(x − m)=true then
        return true;
    end if
end for
return false;
```

When it receives a lane-change demand, $\mathscr{A}_i$ determines whether to change lanes to the adjacent lane based on the collision-avoidance condition on the left side of (15). If a lane change is possible, $\mathscr{A}_i$ sets $\hat{\delta}_{\mathscr{A}}(t,i)$ to change lanes to the adjacent lane. If a lane change is impossible, $\mathscr{A}_i$ sets the ID of the nearest vehicle behind the adjacent lane to $r_d(t,i)$ and sends a deceleration demand to $\mathscr{A}_{r_d(t,i)}$. If the target vehicle is already part of the vehicle group, the deceleration demand is rejected. Thus, for $\xi(t,i)$, $r_d(t,i)$ satisfies

$$\begin{aligned}&\neg\left((r_d(t,i)\neq r_d(t-1,i))\wedge(r_d(t,i)\neq 0)\right)\\&\vee\left(\xi\left(t,r_d(t,i)\right)=0\right)\end{aligned}. \tag{17}$$

If $r_d(t,i) \neq 0$, then $\mathscr{A}_{r_d(t,i)}$ is added to the vehicle group as the assistant vehicle. The front and assistant vehicles are split from the traffic congestion only by communication. Therefore, $r_c(t)$ and $r_d(t)$ satisfy

$$\neg\left(r_c(t+1)=0\right) \vee \left(r_c(t)=0 \vee g_c(t,i)=1\right), \tag{18}$$

$$\neg\left(r_d(t+1)=0\right) \vee \left(r_d(t)=0 \vee g_c(t,i)=1\right). \tag{19}$$

Based on whether acceleration is possible in the current lane and the lane change demand $r_c(t,i)$, $\mathscr{A}_i$ determines the target moving cell $\hat{\delta}_{\mathscr{A}}(t,i)$ at time t. After determining the target moving cell, $\mathscr{A}_i$ sets the moving probability $p(t,i)$ in accordance with the deceleration demand $r_d(t,j,i)$ of the surrounding vehicles as follows:

$$p(t,i) \leftarrow \begin{cases} p_d & \left(\begin{array}{c}\text{if } \exists j \in \mathscr{I}, \\ \text{s. t. } (r_d(t,j)=i)\end{array}\right) \\ p_{\max}(i) & \text{otherwise} \end{cases}. \tag{20}$$

After setting the movement probability $p(t,i)$, $\mathscr{A}_i$ moves according to Algorithm 3.

$$r_a(t,i) \leftarrow \begin{cases} 0 & (\text{if } g_c(t,i)=1) \\ \varepsilon_{\mathscr{N}}(t,\hat{\delta}_{\mathscr{A}}(t,i)) & \left(\begin{array}{c}\text{else if} \\ \xi(t,\varepsilon_{\mathscr{N}}(t,\hat{\delta}_{\mathscr{A}}(t,i)))=1\end{array}\right) \\ r_a(t-1,i) & \text{otherwise} \end{cases} \tag{21}$$

At this time, $\mathscr{A}_i$ sets the acceleration demand $r_a(t,i)$ according to lines 3–8 of Algorithm 3. The condition of the if statement in line 3 of Algorithm 3 matches the left-hand side of (15). If $r_a(t,i) \neq 0$, then $\mathscr{A}_i$ is added to the vehicle group as a follow vehicle. Next, $\mathscr{A}_i$ updates $\xi(t+1,i)$ based on the movement result and separates the vehicle group. A vehicle separates from the vehicle group when its lane change, deceleration, or acceleration demand is satisfied. The algorithm for updating $\xi(t+1,i)$ is given by Algorithm 4. Line 3 of Algorithm 4 indicates that when $\mathscr{A}_i$ changes lanes based on a lane-change demand, the current vehicle is notified. Line 5 indicates that when $\mathscr{A}_i$ changes lanes, the assistant vehicle, which receives the deceleration demand, and the current vehicle, which issues the lane-change demand, are notified of the completion of the lane change and separation of the two vehicles.

By using $r(t,i)$ and $g_c(t,i)$, $\mathscr{A}_i$ obtains $\xi(t+1,i)$, which is given by

$$\begin{array}{l}\left(\xi(t+1,i)=0\right) \equiv \\ \left(r(t,i)=0 \wedge \left(r(t,j)\neq i, \forall j \in I\right)\right) \vee \left(g_c(t,i)=1\right).\end{array} \tag{22}$$

Thus, in accordance with (6) and (22), a vehicle group is formed by the current, front, assistant, and follow vehicles. If $r(t,i) \neq 0$, then $\mathscr{A}_i$ merges into the vehicle group. Otherwise, $\mathscr{A}_i$ separates from the vehicle group. Additionally, if $\mathscr{A}_i$ demands another vehicle to change lanes, decelerate, or accelerate (i.e., $r(t,i) \neq 0$), $\mathscr{A}_i$ will maintain $r(t,i)$ until the demand is fulfilled. Subsequently, $\xi(t+1,i)$ and $r(t+1,i)$ satisfy

$$\neg\left(\xi(t+1,i)=1\right) \vee \left(\begin{array}{c}\left(r_c(t+1)=r_c(t)\right) \\ \wedge\left(r_d(t+1)=r_d(t)\right) \\ \wedge\left(r_a(t+1)=r_a(t)\right)\end{array}\right). \tag{23}$$

Algorithm 3 Moving agents

1: Set x and y from $v_y^x = \hat{\delta}_{\mathscr{A}}(t,i)$;
2: **if** $(\text{rand}() < p(t,i))$ **then**
3: **if** $\left(\begin{array}{c}\sum_{j\in(\mathscr{I}\setminus\{i\})} \varepsilon\left(t,j,v_y^x\right) \\ +\varepsilon\left(t,j,v_{y-1}^x\right)=1\end{array}\right)$ **then**
4: $\delta_{\mathscr{A}}(t,i) \leftarrow \varepsilon_{\mathscr{A}}(t,i)$;
5: **if** $\xi\left(t,\varepsilon_{\mathscr{N}}(t,\hat{\delta}_{\mathscr{A}}(t,i))\right)=1$ **then**
6: $r_a(t,i) \leftarrow \varepsilon_{\mathscr{N}}\left(t,\hat{\delta}_{\mathscr{A}}(t,i)\right)$;
7: **end if**
8: **else**
9: $\delta_{\mathscr{A}}(t,i) \leftarrow \hat{\delta}_{\mathscr{A}}(t,i)$;
10: **end if**
11: **else**
12: $\delta_{\mathscr{A}}(t,i) \leftarrow \varepsilon_{\mathscr{A}}(t,i)$;
13: **end if**

Algorithm 4 Separation of vehicle groups

1: Set x and y from $v_y^x = \varepsilon_{\mathscr{A}}(t,i)$;
2: **if** $(\exists j \in \mathscr{I} \ \ s.t. \ \ r_c(t,j)=i)$ **then**
3: **if** $\left(\ \left(\delta_{\mathscr{A}}(t,i)=v_y^{x+1}\right) \vee \left(\delta_{\mathscr{A}}(t,i)=v_y^{x-1}\right)\ \right)$ **then**
4: $g_c(t,j) \leftarrow 1$;
5: **if** $(r_d(t,i)\neq 0)$ **then**
6: $g_c(t+1,i) \leftarrow 1$;
7: $g_c(t+1,r_d(t,i)) \leftarrow 1$;
8: **end if**
9: **end if**
10: **else if** $(r_a(t,i)\neq 0)$ **then**
11: **if** $\left(\begin{array}{c}\left(\delta_{\mathscr{A}}(t,i)=\hat{\delta}_{\mathscr{A}}(t,i)\right) \\ \wedge\left(\xi\left(t,r_a(t,i)\right)=0\right)\end{array}\right)$ **then**
12: $g_c(t,i) \leftarrow 1$;
13: **end if**
14: **end if**

V. DEMAND-FOR GRAPHS OF TRAFFIC CONGESTION

In this section, we present the demand-for graphs of traffic congestion, which we initially proposed in [23].

The demand-for graphs can be used to evaluate the size of traffic congestion based on the demand for cooperative control and deceleration agents. The pausing and deceleration of an agent implies a reduction in the flow rate of the entire search system. Therefore, we propose a congestion-evaluation method based on the demands for cooperative control made by individual agents to prevent them from pausing and decelerating.

The demand-for graph at time t is denoted as $G_d(t) = (V_d, E_d(t))$, where $V_d : \{n_1, n_2, \cdots, n_I\}$ are the nodes representing the vehicles, $E_d(t)$ are the edges representing the demands between the vehicles, and $n_i \in V_d$ is the node corresponding to $\mathscr{A}_i$. Additionally, $(n_i, n_j) \in E_d(t)$ represents demand from $\mathscr{A}_i$ to $\mathscr{A}_j$ at time t.

A. CONVENTIONAL TRAFFIC CONGESTION

In this subsection, we present the demand-for graph of conventional congestion due to traffic concentration as described in [14]–[19]. For conventional traffic congestion, $G_d(t)$ is given by

$$E_d(t) \leftarrow \bigcup_{i\in I}\bigcup_{j\in(I\setminus\{i\})} f_1(t,i,j), \tag{24}$$

$$f_1(t,i,j) = \begin{cases} (n_i,n_j) & \left(\text{if } \varepsilon_{\mathscr{N}}\left(t,\hat{\delta}_{\mathscr{A}}(t,i)\right)=j\right) \\ \emptyset & \text{otherwise} \end{cases}.$$

In this case, if $\varepsilon_{\mathscr{N}}\left(t,\hat{\delta}_{\mathscr{A}}(t,i)\right)=j$, then $\mathscr{A}_i$ pauses according to (12). Based on (12) and (24), $(n_i,n_j)\in E_d(t)$ implies that $\mathscr{A}_i$ is decelerating owing to conventional congestion.

B. ALTRUISTIC CONGESTION

Next, we present the demand-for graph of altruistic congestion. For this type of congestion, $G_d(t)$ is expressed as

$$E_d(t) \leftarrow \bigcup_{i\in I}\bigcup_{j\in(I\setminus\{i\})} f_2(t,i,j), \tag{25}$$

$$f_2(t,i,j) = \begin{cases} (n_i,n_j) & (\text{if } r(t,i)=j) \\ \emptyset & \text{otherwise} \end{cases}.$$

Fig. 4 and Fig. 5 show an example of an altruistic lane change and the corresponding demand-for graph, respectively, where the boxed line represents the vehicle group involved in the altruistic lane change. Furthermore, in Fig. 5, (n_1,n_3) represents the lane-change demand made by $\mathscr{A}_1$ to $\mathscr{A}_3$ shown in Fig. 4; (n_3,n_2) represents the deceleration demand made by $\mathscr{A}_3$ to $\mathscr{A}_2$; (n_5,n_2), (n_7,n_6), and (n_6,n_1) represent the acceleration demands. The decelerations of the assistant and follow vehicles cause altruistic congestion. Therefore, we consider the edges in $G_d(t)$ to be of altruistic congestion.

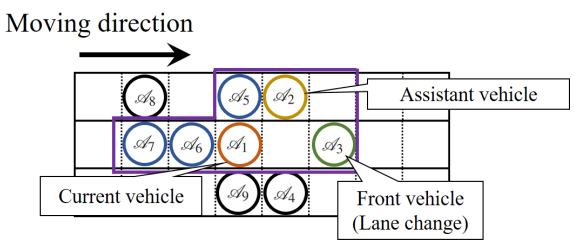

FIGURE 4: Grouping for altruistic lane change

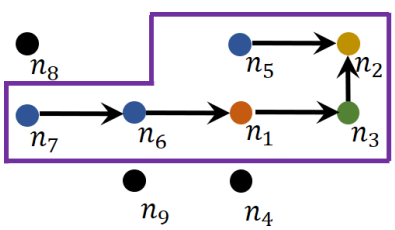

FIGURE 5: Demand-for graph

C. SIZE OF CONGESTION

Herein, the beginning of traffic congestion is defined by the vehicle corresponding to the endpoint n_i, which has a zero outgoing order on the demand-for graph. Based on (24), if $\mathscr{A}_i$ is located at the beginning of the traffic congestion, then $r(t,i)=0$ is valid. We also define the distance between the endpoints in the demand-for graph as the length of the traffic congestion. The distance between the nodes in the graph indicates the length of the shortest path connecting the two nodes. Equations (22) and (24) reveal that the length of the traffic congestion represents the number of demands that the vehicle at the tail end of the traffic congestion needs to fulfill to be able to separate from the vehicle group. Therefore, the time required to completely resolve the traffic congestion is proportional to the length of the congestion.

VI. STATE-TRANSITION EQUATIONS OF DEMAND-FOR GRAPHS

Here, we derive the state-transition equations of the adjacency matrix corresponding to the demand-for graph proposed in [23]. Subsequently, we derive new proofs for the altruistic congestion theorems presented in [23] using the derived equations and discuss the characteristics of these theorems.

In this section, we present a method for evaluating the expansion and resolution speeds of congestion based on the time variation of the adjacency matrix. This matrix corresponds to the demand-for graph related to the scale of the congestion, which is discussed in Section 5. We denote the adjacency matrix of the demand-for graph at time t as $\boldsymbol{\Phi}(t)\in\{0,1\}^{I\times I}$. Then, we denote the state transition of $\boldsymbol{\Phi}(t)$ as

$$\boldsymbol{\Phi}(t+1) = \boldsymbol{B}\boldsymbol{u}_1(t) - \boldsymbol{D}\boldsymbol{u}_2(t). \tag{26}$$

In Equation (26), $\boldsymbol{u}_1(t)$ denotes the issuance of an action demand associated with an altruistic lane change; $\boldsymbol{u}_2(t)$ represents the fulfillment of the action demand by the agent; and $\boldsymbol{B}$ and $\boldsymbol{D}$ are the input matrices that represent the changes in the demand-for graphs corresponding to $\boldsymbol{u}_1(t)$ and $\boldsymbol{u}_2(t)$, respectively. The setting of $\boldsymbol{B}$ and $\boldsymbol{u}_1(t)$ allows the expansion in the size of the congestion to be defined and observed, whereas the setting of $\boldsymbol{D}$ and $\boldsymbol{u}_2(t)$ allows the size of the congestion due to cooperative and non-cooperative behavior to be defined and observed.

A. CONVENTIONAL TRAFFIC CONGESTION

From Equation (24), we derive the adjacency matrix of the demand-for graph shown in Equation (26) corresponding to

conventional congestion, as follows:

$$\boldsymbol{u}_1(t) = \begin{bmatrix} \boldsymbol{U}_1(t,1) \\ \vdots \\ \boldsymbol{U}_1(t,I) \end{bmatrix}, \tag{27}$$

$$\boldsymbol{U}_1(t,i) = \begin{bmatrix} f_3(t,i,1) & 0 & \cdots & 0 \\ 0 & f_3(t,i,2) & \ddots & \vdots \\ \vdots & \ddots & \ddots & 0 \\ 0 & \cdots & 0 & f_3(t,i,I) \end{bmatrix},$$

$$f_3(t,i,j) = \begin{cases} 1 & \left(\text{if } \varepsilon_{\mathscr{N}}(t,\hat{\delta}_{\mathscr{A}}(t,i)) = j\right) \\ 0 & \text{otherwise} \end{cases},$$

$$\boldsymbol{B} = \begin{bmatrix} \boldsymbol{1}_I{}^{\mathrm{T}} & \boldsymbol{0}_I{}^{\mathrm{T}} & \cdots & \boldsymbol{0}_I{}^{\mathrm{T}} \\ \boldsymbol{0}_I{}^{\mathrm{T}} & \boldsymbol{1}_I{}^{\mathrm{T}} & \ddots & \vdots \\ \vdots & \ddots & \ddots & \boldsymbol{0}_I \\ \boldsymbol{0}_I{}^{\mathrm{T}} & \cdots & \boldsymbol{0}_I{}^{\mathrm{T}} & \boldsymbol{1}_I{}^{\mathrm{T}} \end{bmatrix}, \tag{28}$$

$$\boldsymbol{u}_2(t) = \begin{bmatrix} \boldsymbol{U}_2(t,1) \\ \vdots \\ \boldsymbol{U}_2(t,I) \end{bmatrix}, \tag{29}$$

$$\boldsymbol{U}_2(t,i) = \begin{bmatrix} f_4(t,i,1) & 0 & \cdots & 0 \\ 0 & f_4(t,i,2) & \ddots & \vdots \\ \vdots & \ddots & \ddots & 0 \\ 0 & \cdots & 0 & f_4(t,i,I) \end{bmatrix},$$

$$f_4(t,i,j) = \begin{cases} f_3(t,i,j) & (\text{if } \delta_{\mathscr{A}}(t,j) \neq \varepsilon_{\mathscr{A}}(t,j)) \\ 0 & \text{otherwise} \end{cases},$$

$$\boldsymbol{D} = \begin{bmatrix} \boldsymbol{1}_I{}^{\mathrm{T}} & \boldsymbol{0}_I{}^{\mathrm{T}} & \cdots & \boldsymbol{0}_I{}^{\mathrm{T}} \\ \boldsymbol{0}_I{}^{\mathrm{T}} & \boldsymbol{1}_I{}^{\mathrm{T}} & \ddots & \vdots \\ \vdots & \ddots & \ddots & \boldsymbol{0}_I \\ \boldsymbol{0}_I{}^{\mathrm{T}} & \cdots & \boldsymbol{0}_I{}^{\mathrm{T}} & \boldsymbol{1}_I{}^{\mathrm{T}} \end{bmatrix}. \tag{30}$$

In Equation (27), $\boldsymbol{U}_1(t,i)$ is a diagonal matrix with $f_3(t,i,j)$ as the j-th row, j-th column elements. In Equation (29), $\boldsymbol{U}_2(t,i)$ is a diagonal matrix with $f_4(t,i,j)$ as the j-th row, j-th column elements, where $f_4(t,i,j)$ indicates whether the action demand made by $\mathscr{A}_i$ to $\mathscr{A}_j$ is fulfilled by the movement of $\mathscr{A}_j$. In Equations (28) and (30), $\boldsymbol{B}$ and $\boldsymbol{D}$ are each defined as a diagonal block matrix with row vector $\boldsymbol{1}_I{}^{\mathrm{T}}$ as the diagonal elements, where $\boldsymbol{I}$ is the number of elements of the vector. In Equations (29) and (30), the i-th row, $\boldsymbol{D}\boldsymbol{u}_2(t)$-th column elements in (26) are the i-th to j-th column elements from $\mathscr{A}_i$ to $\mathscr{A}_j$ by moving the parcel of $\mathscr{A}_j$. Equations (26), (27), and (29) satisfy

$$\boldsymbol{u}_2(t) \leq \boldsymbol{u}_1(t). \tag{31}$$

Meanwhile, in Equations (28) and (30), $\boldsymbol{u}_1(t) - \boldsymbol{u}_1(t-1)$ and $\boldsymbol{u}_2(t)$ denote the increase in and elimination of traffic congestion, respectively, when $\boldsymbol{B} = \boldsymbol{D}$ in Equation (26).

B. ALTRUISTIC CONGESTION

From Equation (25), we derive $\boldsymbol{u}_1(t)$ under altruistic congestion as follows:

$$\boldsymbol{u}_1(t) = \begin{bmatrix} \boldsymbol{U}_1(t,1) \\ \vdots \\ \boldsymbol{U}_1(t,I) \end{bmatrix}, \tag{32}$$

$$\boldsymbol{U}_1(t,i) = \begin{bmatrix} f_5(t,i,1) & 0 & \cdots & 0 \\ 0 & f_5(t,i,2) & \ddots & \vdots \\ \vdots & \ddots & \ddots & 0 \\ 0 & \cdots & 0 & f_5(t,i,I) \end{bmatrix},$$

$$f_5(t,i,j) = \begin{cases} 1 & \left(\text{if } \begin{pmatrix} \delta_{\mathscr{A}}(t,i) = \hat{\delta}_{\mathscr{A}}(t,i) \\ \wedge \xi(t,i) \neq 0 \end{pmatrix} \vee (r_c(t,i) = j) \vee (r_d(t,i) = j)\right) \\ 0 & \text{otherwise} \end{cases},$$

and $\boldsymbol{u2}$ as follows:

$$\boldsymbol{u}_2(t) = \begin{bmatrix} \boldsymbol{U}_2(t,1) \\ \vdots \\ \boldsymbol{U}_2(t,I) \end{bmatrix}, \tag{33}$$

$$\boldsymbol{U}_2(t,i) = \begin{bmatrix} f_6(t,i,1) & 0 & \cdots & 0 \\ 0 & f_6(t,i,2) & \ddots & \vdots \\ \vdots & \ddots & \ddots & 0 \\ 0 & \cdots & 0 & f_6(t,i,I) \end{bmatrix},$$

$$f_6(t,i,j) = \begin{cases} f_5(t,i,j) g_c(t,i) & (\text{if } r_a(t,j) = 0) \\ f_5(t,i,j)\,(1 - f_3(t,i)) & \text{otherwise} \end{cases}.$$

Meanwhile, $\boldsymbol{B}$ and $\boldsymbol{D}$ are given by Equations (28) and (30), respectively. In this case, for Equations (32) and (33), $f_5(t,i,j)$ satisfies

$$(f_5(t,i,j) = 1) \equiv \begin{pmatrix} f_3(t,i,j) = 1 \vee r_c(t,i) = j \\ \vee r_d(t,i) = j \end{pmatrix}. \tag{34}$$

The lane-change demands represented by $r_c(t,i)$ and the deceleration demand represented by $r_d(t,i)$ are both action demands for cooperative behavior that require communication. Equations (32) and (34) constitute an altruistic lane change by a CAV. An increase in traffic congestion, which originates from the two coordinated actions required for lane change and deceleration, can be observed. The two cooperative actions in Equation (33) satisfy the following conditions:

$$(f_6(t,i,j) = 1) \equiv f_4(t,i,j) = 1 \vee g_c(t,i) = 1. \tag{35}$$

Equation (35) indicates that the traffic congestion shown in Equation (33) is naturally resolved because of the communicated information $g_c(t,i)$ that represents the cooperative actions. Therefore, a demand-for graph of the congestion based on Equations (32) and (33) can be used to reevaluate the changes in the size of the congestion due to the issuance and fulfillment of action demands to achieve cooperative behavior.

In this case, Equations (32) and (33) prove that Equation (31) is valid. Therefore, $\boldsymbol{u}_1(t) - \boldsymbol{u}_1(t-1)$ and $\boldsymbol{u}_2(t)$

correspond to expansion and reduction in the congestion, respectively.

VII. MAIN RESULTS

In this study, we consider the expected reduction in the length of traffic congestion at time t as the resolution speed $\sigma_{rl}(t)$ of this congestion, and thus, $\sigma_{rl}(t)$ satisfies *Theorem 1*.

Theorem 1. *All front vehicles are assumed to have completed the altruistic lane change at time $t-1$. In this case, $\sigma_{rl}(t)$ is equal to the movement probability of the second vehicle from the beginning of the traffic congestion.*

Proof. Based on assumptions (5), (18), and (19), $r_c(t,i)$ and $r_d(t,i)$ satisfy

$$r_c(t,i) = r_d(t,i) = 0, \quad \forall i \in \mathscr{I}. \tag{36}$$

In this case, the vehicle at the beginning of a traffic congestion is a follow vehicle. Let i' be the ID of the follow vehicle at the beginning of the altruistic congestion. Based on Equations (32), (33), and (36), $\boldsymbol{u}_2(t)$ satisfies

$$f_6(t,i,j) = f_5(t,i,j)\left(1 - f_3(t,i)\right). \tag{37}$$

Based on Algorithm 4 and Equation (22), $r_a(t,i')$ satisfies

$$\begin{aligned} &\neg\left(r_a(t,i') > 0 \wedge g_c(t,i') = 1\right) \\ &\vee \delta\left(t, r_a(t,i')\right) = \hat{\delta}_{\mathscr{A}}(t, r_a(t,i')). \end{aligned} \tag{38}$$

Equation (38) is revised for $\mathscr{A}_j$, as follows:

$$\begin{aligned} &\neg\left(r_a(t,j) = i'\right) \\ \vee &\left(g_c(t,j) = 0 \wedge \sum_{i \in \mathscr{I}} \varepsilon(t+1, i, \varepsilon_{\mathscr{A}}(t, r_a(t,i'))) = 0\right). \end{aligned} \tag{39}$$

Based on Equations (32), (33), (37), and (39), the $\sigma_{rl}(t)$ of $\mathscr{A}_{i'}$ at the beginning of altruistic congestion is obtained as follows:

$$\sigma_{rl}(t) = p(t,i'). \tag{40}$$

□

Theorem 1 reveals that after the front vehicle changes lanes, the agent separates from the traffic congestion. In this case, the beginning of the traffic congestion shifts to the inlet side over time. This is consistent with traffic congestion due to traffic concentration as reported in [19].

Next, we describe the conditions for the reduction in altruistic congestion. Notably, $\sigma_{rl}(t)$ satisfies *Theorem 2*.

Theorem 2. *If the front vehicle does not change lanes, then $\sigma_{rl}(t) = 0$.*

Proof. Let i' be the ID of the front vehicle located at the beginning of the traffic congestion. Consider the situation in which $\mathscr{A}_{i'}$ does not change lanes: In this case, based on Algorithm 4, $g_c(t,i)$ for the current and assistant vehicles satisfies

$$\neg\left(r_c(t,i) = i' \vee r_d(t,i') = i\right) \vee g_c(t,i) = 0. \tag{41}$$

Based on Equations (33), (41) and Algorithm 4, $g_c(t,i)$ for the follow vehicle satisfies

$$\neg r_a(t,i) = r(t,i) \vee g_c(t,i) = 0. \tag{42}$$

Based on Equations (41) and (42), $g_c(t,i)$ satisfies

$$g_c(t,i) = 0, \quad \forall i \in \mathscr{I}. \tag{43}$$

Based on Equation (33), $\sigma_{rl}(t)$ and $\boldsymbol{u}_2(t)$ satisfy

$$\sigma_{rl}(t) > 0 \equiv \exists\{i,j\} \subset \mathscr{I}, \text{s. t. } \left(f_6(t,i,j) = 1\right). \tag{44}$$

Based on Equations (33), (43), and (44), if and only if $\sigma_{rl}(t) > 0$, then one of the following equations is satisfied:

$$\xi(t,i) \neq 0 \wedge r_a(t) = 0 \wedge g_c(t,i,j) = 1, \tag{45}$$

$$\xi(t, r(t,i)) = 0 \wedge r_a(t) \neq 0. \tag{46}$$

However, Equation (43) reveals that Equation (45) is not satisfied. In addition, Equations (21), (22), and (43) indicate that Equation (46) is not satisfied. Therefore, if the front vehicle does not change lanes, then $\sigma_{rl}(t) = 0$ and $\boldsymbol{u}_2(t) = \boldsymbol{0}$. □

Theorem 2 shows that before the altruistic lane change of the front vehicle, $\sigma_{rl}(t)$ is 0. In this case, the vehicles at the beginning of the altruistic congestion continue to move to the outlet without separating from the traffic congestion.

Based on *Theorem 1* and *Theorem 2*, the altruistic congestion is reduced if and only if the front vehicle changes lanes in response to the lane-change demand. From *Theorem 1* and *Theorem 2*, we expect that a stationary position exists at the beginning of traffic congestion owing to altruistic lane changes. In this case, the inlet and outlet sides exhibit high and low densities, respectively. This is an inversion of the phase separation of the density owing to intersections in the serial networks of the ASEPs for the existing congestion as reported in [19]. From *Theorem 1* and *Theorem 2*, we identify the traffic-flow characteristics of CAVs that change lanes as a cooperative function, i.e., a high density of vehicles is observed owing to congestion on the inlet side, and the speeds of the vehicles increase owing to traffic smoothing on the outlet side.

VIII. NUMERICAL RESULTS

This section presents an evaluation of the effects of the reduction in traffic flow due to altruistic congestion and the increase in traffic flow due to traffic facilitation owing to the acceleration of the current vehicle after a lane change.

A. SIMULATION LAYOUT

Fig. 6 shows the multi-lane ASEP used in the numerical experiments conducted in this study.

Fig. 6 is a multi-lane ASEP with number of lanes $X = 2$ and length $Y = 100$. The top-left corner of Fig. 6 shows v_1^1, and the bottom-right corner shows v_{100}^2. Of these, v_1^x is the inlet of a single path; if no vehicle is present, a new vehicle is created with a probability of 0.5. On the other hand, v_{100}^x is the outlet of a single path, and the vehicle in v_{100}^x at time t will

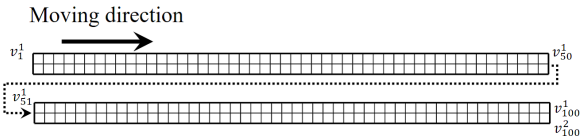

FIGURE 6: Simulation layout

disappear at time $t+1$. In this experiment, the speed of the agent is varied in two steps, i.e., 0.3 and 0.9. The speed when decelerating for a lane change is set to $p_d = 0.1$. The ratio of the vehicle speeds of each new vehicle is 1:2 for steps 0.3 and 0.9. In these experiments, $p(t,i)$ is applicable to $\mathscr{A}_i$ moving forward. If $\mathscr{A}_i$ attempts to change lanes, $\mathscr{A}_i$ will move to the adjacent cell, except under the pause condition, according to Equation (15).

B. EVALUATION OF TRAFFIC CONGESTION

In [8], congestion relief due to altruistic lane changes was evaluated. These lane changes involve increased vehicle speeds due to the communications between vehicles. In [26], [27], congestion due to multi-lane traffic flow was evaluated by comparing the time trends of the density distributions according to the lanes.

Theorem 1 proposed in this study shows that altruistic congestion is resolved by the movement of the agent after a lane change by the front vehicle. Thus, traffic congestion occurs at the inlet and is resolved owing to the movement of the agent. If the flow rate of the traffic is almost constant, the density of agents is expected to be higher and lower on the inlet and outlet sides, respectively. Therefore, this study evaluates the density of agents, traffic flow rates, and vehicle speeds relative to the travel distances of the agents. To compare the inlet and outlet densities of a multi-lane ASEP, we propose a new method for evaluating these densities based on the integrated flow rate and the average flow velocity in the observation interval Ts.

We denote the average density between times t and $t+T_s$ in cell $v_y^x \in \mathscr{N}$ as $\rho(t,T_s,v_y^x)$ $(0 \le \rho(t,T_s,v_y^x)) \le 1)$, and the average flow rate over the entire search area as $Q(t,T_s,v_y^x)$ $(0 \le Q(t,T_s,v_y^x) \le 1)$. We derive $Q(t,T_s,v_y^x)$ as follows:

$$Q(t,T_s,v_y^x) = \sum_{s=0}^{T_s-1} \sum_{i\in I} \varepsilon(t+s-1,i,v_y^x)\left(1-\varepsilon(t+s,i,v_y^x)\right). \tag{47}$$

In Equation (47), $\varepsilon\left(t-1,i,v_y^x\right) = 1$ denotes that at time $t-1$, $\mathscr{A}_i$ is present in v_y^x. Similarly, $\varepsilon\left(t,i,v_y^x\right) = 0$ denotes that at time t, $\mathscr{A}_i$ is not present in v_y^x. In this case, $\varepsilon\left(t-1,i,v_y^x\right)\left(1-\varepsilon\left(t,i,v_y^x\right)\right) = 1$ indicates that the $\mathscr{A}_i$ present in v_y^x at time $t-1$ has made a parcel move. Therefore, Equation (47) represents the number of agents that have passed through v_y^x during the observation period T_s.

We denote the average speed of the agents between times t and $t+T_s$ in cell $v_y^x \in \mathscr{N}$ as $v(t,T_s,v_y^x)$ $(0 \le v(t,T_s,v_y^x)) \le 1)$. In this study, we express the speed of the agent in terms of movement probability p. Therefore, we derive $v\left(t,T_s,v_y^x\right)$ as follows:

$$\begin{aligned} v(t,T_s,v_y^x) &= \frac{\sum_{s=0}^{T_s-1}\sum_{i\in I}\varepsilon(t+s-1,i,v_y^x)\left(1-\varepsilon(t+s,i,v_y^x)\right)}{\sum_{s=0}^{T_s-1}\sum_{i\in I}\varepsilon(t+s,i,v_y^x)} \\ &= \frac{Q(t,T_s,v_y^x)}{\sum_{s=0}^{T_s-1}\sum_{i\in I}\varepsilon(t+s,i,v_y^x)}. \end{aligned} \tag{48}$$

In Equation (48), the denominator denotes the cumulative number of agents in v_y^x. Therefore, $v(t,T_s,v_y^x)$ is the reciprocal of the average number of steps during which the agents remain in v_y^x. Because the flow rate is the product of density and speed, we derive $\rho\left(t,T_s,v_y^x\right)$ from Equations (47) and (48) as follows:

$$\rho(t,T_s,v_y^x) = \frac{Q(t,T_s,v_y^x)}{T_s v\left(t,T_s,v_y^x\right)} = \frac{\sum_{s=0}^{T_s-1}\sum_{i\in I}\varepsilon(t+s,i,v_y^x)}{T_s}. \tag{49}$$

C. TEMPORARY TRAFFIC CONGESTION

First, we conducted an experiment in which traffic congestion was generated owing to a low-speed vehicle and then resolved. In this experiment, the opening of the inlet was terminated at time $t = 200$, and changes in the density of the agents in the multi-lane ASEP were observed up to time $t = 1000$. Furthermore, the density of vehicles on the road after altruistic lane changes (target distance $d = 2$) was compared with that without altruistic lane changes. Even in the case of no altruistic lane changes, agents change lanes for self-acceleration in accordance with Algorithms 1 and 2.

We demonstrate that $\rho\left(t,20,v_y^x\right)$ corresponds to Lanes 1 and 2 in Fig. 7 and Fig. 8, respectively. These figures show that the all agents reach the end of the ASEP for both Lanes 1 and 2 in the absence of altruistic lane changes within time $t = 700$.

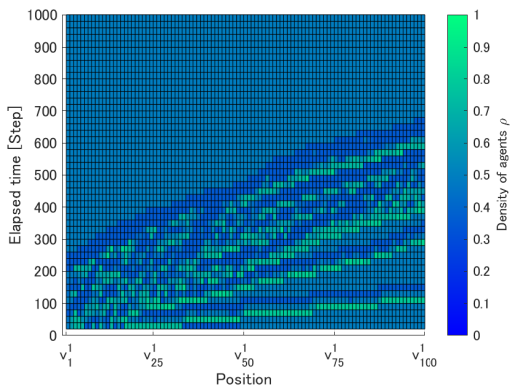

FIGURE 7: Simulation results obtained for Lane 1 (without altruistic lane changes)

Next, we present the traffic congestion generated when a lane change is made at a target distance of $d = 2$. Similar to the case without any lane changes, the opening of the inlet was terminated at time $t = 200$, and changes in the density of the agents in the multi-lane ASEP were observed up to

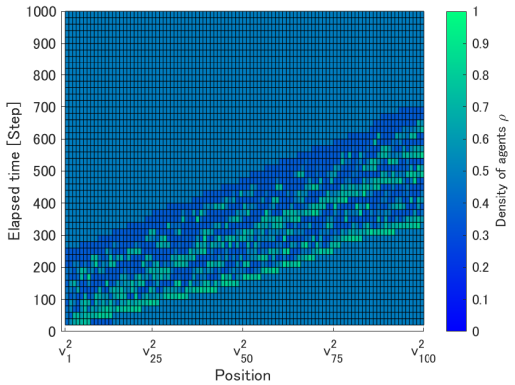

FIGURE 8: Simulation results obtained for Lane 2 (without altruistic lane changes)

time $t = 1000$. We demonstrate that $\rho\left(t, 20, v_y^x\right)$ corresponds to Lanes 1 and 2 in Fig. 9 and Fig. 10, respectively. In Fig. 10, some agents remain only in Lane 2 of the ASEP at time $t = 700$, owing to the altruistic lane changes.

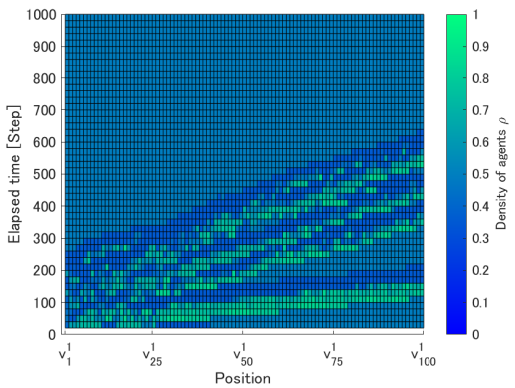

FIGURE 9: Simulation results obtained for Lane 1 (with altruistic lane changes)

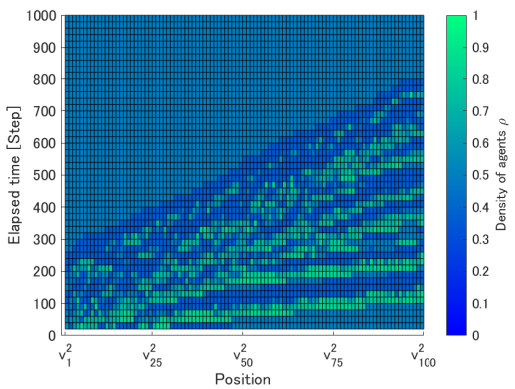

FIGURE 10: Simulation results obtained for Lane 2 (with altruistic lane changs)

Fig. 9 and Fig. 10 reveal the altruistic lane changes caused by lane segmentation according to vehicle speed. However, this experiment did not clarify the lane-by-lane speed changes or the impact of new altruistic congestion on the density at the inlet side.

D. STEADY FLOW

Next, we conducted a numerical experiment to determine the flow-velocity variation under steady-state flow. This experiment evaluated the congestion generated as a result of altruistic lane changes on the inlet side and the reduction in this congestion after lane changes based on the changes in flow velocity in each compartment. In this experiment, the probability of an agent being present at the inlet was set to 0.1.

First, we demonstrate that steady-state flow is achieved in the absence of altruistic lane changes. Agents change lanes for self-acceleration in accordance with Algorithms 1 and 2. In this experiment, a steady flow was generated by repeatedly moving the vehicle until the 3900th step. Subsequently, $\rho\left(3900, 100, v_y^x\right)$ and $Q\left(3900, 100, v_y^x\right)$ were observed up to time $t = 4000$. On the other hand, $v\left(3900, 100, v_y^x\right)$ without lane changes is shown in Fig. 11. Fig. 11 reveals that no differences occurred in the lane-by-lane flow velocities when no altruistic lane changes were performed. The average flow velocities in Lanes 1 and 2 were 0.272 and 0.274, respectively.

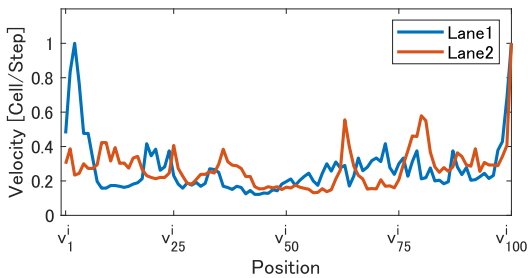

FIGURE 11: Simulation results (without altruistic lane changes)

Next, we demonstrate that a steady-state flow can be achieved through lane changes. In the experiment, a steady flow was generated by repeatedly moving the vehicle during the 3900th step, and $\rho\left(3900, 100, v_y^x\right)$ and $Q\left(3900, 100, v_y^x\right)$ were observed up to time $t = 4000$. The resulting $v\left(3900, 100, v_y^x\right)$ due to lane changes is shown in Fig. 12.

As shown in Fig. 12, the flow velocity increases from the inlet to the outlet side. This result is consistent with the inversion of the congestion and free phases in altruistic congestion, which we derive from Theorems 1 and 2 in Section 7. This result shows that altruistic lane changes by CAVs cause flow reduction at the inlet due to altruistic congestion and flow increases at the outlet due to traffic facilitation.

On the other hand, Fig. 12 shows that throughout the multi-lane ASEP, the velocities in Lane 1 were higher than those in

Lane 2 owing to altruistic lane changes. The average flow velocity in Lane 1 was 0.628 and that in Lane 2 was 0.147. The average flow velocity for the overall ASEP was 0.388, which exceeded that in the absence of altruistic lane changes. Now, we compare these results with the flow velocity in the maximum flow phase. The flow velocity in the maximum flow phase is obtained to be $(1-\sqrt{1-p})$, where p denotes the moving probability. Thus, the speed of a low-speed vehicle in the maximum flow phase is 0.163, whereas the speed of a high-speed vehicle is 0.684. In this experiment, the reduction in the average speed compared to that in the maximum flow phase owing to altruistic congestion was less than 10%. This result indicates that altruistic lane changes are effective at reducing traffic congestion.

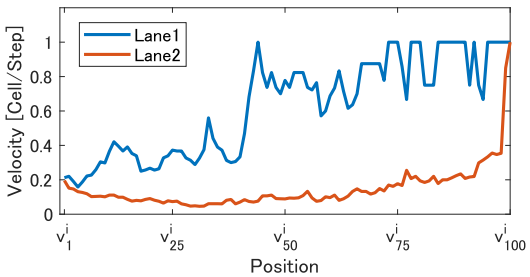

FIGURE 12: Simulation results (with altruistic lane changes: $d = 2$)

The results show that lane separation according to speed owing to altruistic lane changes is effective at reducing the overall congestion in a multi-lane ASEP. A comparison between the flow velocities on the inlet and outlet sides clarified the occurrence and reduction of new traffic congestion owing to the introduction of cooperative functions.

IX. CONCLUSIONS

This study focuses on lane changes performed by CAVs for traffic facilitation. We evaluated the congestion generated as a result of altruistic lane changes by CAVs and discussed the characteristics of this congestion. In this study, we modeled the search behaviors of vehicles as a multi-lane ASEP search to determine the traffic flow, including lane changes, and evaluate the impact of the generated congestion on the traffic flow rate. To evaluate the size of the altruistic congestion and reduction speed based on agent behavior, we used demand-for graphs, which is a method initially proposed in [23], to represent the congestion.

Here, we derived the state-transition equations corresponding to the adjacency matrix of the demand-for graph related to altruistic congestion. The main contribution of this study is that it compared the characteristics of altruistic congestion with those of conventional congestion caused by traffic concentration. This was achieved by obtaining another proof of the necessary condition for resolving congestion using the derived state-transition equations. In addition, we validated the characteristics of altruistic traffic congestion via numerical experiments.

The contribution of this study is the visualization of the characteristics of altruistic congestion generated as a result of the cooperative behaviors of CAVs through the inversion of the congestion and free phases from conventional congestion. This will enable the trade-off between the decrease in the traffic flow rate due to altruistic congestion and the traffic facilitation due to the CAVs to be evaluated.

The results of the numerical experiments have shown that altruistic congestion occurs at the inlet and is resolved at the outlet owing to traffic facilitation. Furthermore, these results reveal that the traffic flow resulting from the traffic facilitation increases at the outlet and decreases owing to altruistic congestion at the inlet.

In this study, the proposed congestion-analysis method was applied to a multi-lane one-way road. In future studies, the use of the proposed method for the congestion analysis of more complex traffic networks will be addressed.

REFERENCES

[1] M. Forster, R. Frank, M. Gerla, and T. Engel: A Cooperative Advanced Driver Assistance System to Mitigate Vehicular Traffic Shock Waves, *IEEE INFOCOM 2014 - IEEE Conference on Computer Communications*, pp. 1968–1976 (2014)

[2] M. Won, T. Park, and S. H. Son: Toward Mitigating Phantom Jam Using Vehicle-to-Vehicle Communication, IEEE Transactions on Intelligent Transportation Systems, Vol. 18, No. 5, pp. 1313–1324 (2017)

[3] N. Goulet and B. Ayalew: Distributed Maneuver Planning with Connected and Automated Vehicles for Boosting Traffic Efficiency, *IEEE Transactions on Intelligent Transportation Systems*, Early access (2021)

[4] D. Li and B. De Schutter: Distributed Model-Free Adaptive Predictive Control for Urban Traffic Networks, *IEEE Transactions on Control Systems Technology*, Vol. 30, No. 1, pp. 180–192 (2022)

[5] Z. Shen, Y. Liu, Z. Li, and M. H. Nabin: Cooperative Spacing Sampled Control of Vehicle Platoon Considering Undirected Topology and Analog Fading Networks, *IEEE Transactions on Intelligent Transportation Systems*, Early access (2022)

[6] H. Zhang, L. Du, and J. Shen: Hybrid MPC System for Platoon Based Cooperative Lane Change Control Using Machine Learning Aided Distributed Optimization, *Transportation Research Part B: Methodological*, Early access, (2021)

[7] F. Tajdari, C. Roncoli, and M. Papageorgiou: Feedback-Based Ramp Metering and Lane-Changing Control with Connected and Automated Vehicles, *IEEE Transactions on Intelligent Transportation Systems*, Vol. 23, No. 2, pp. 939–951 (2022)

[8] N. Wang, X. Wang, P. Palacharla, and T. Ikeuchi: Cooperative Autonomous Driving for Traffic Congestion Avoidance through Vehicle-to-Vehicle Communications, *IEEE Vehicular Networking Conference (VNC)*, pp. 327–330 (2017)

[9] Y. Jiang, H. Cong, Y. Wang, Y. Wu, H. Li, Z. Yao: A New Control Strategy of CAVs Platoon for Mitigating Traffic Oscillation in a Two-lane Highway, *Phys. Stat. Mech*, https://doi.org/10.1016/j.physa.2023.129289 (2023)

[10] Y. Wang, Y. Jiang, Y. Wu, Z. Yao: Mitigating traffic oscillation through control of connected automated vehicles: A cellular automata simulation, *Expert Systems with Applications*, https://doi.org/10.1016/j.eswa.2023.121275 (2024)

[11] D. Lee, S. Lee, Z. Chen, B. Brian Park, and D. H. Shim: Design and Field Evaluation of Cooperative Adaptive Cruise Control with Unconnected Vehicle in the Loop, *Transportation Research Part C: Emerging Technologies*, Vol. 132, p. 103364 (2021)

[12] K. Iida, Y. Wadasaki, M. Tada, T. Chikugo, S. AN, H. Sawada, and Y. Kinosada: Evaluation of Safety and Efficiency of Traffic Flow with Different Proportion of ACC Vehicles, *JSTE Journal of Traffic Engineering*, Vol. 4, No. 1, pp. A238—A245 (2018)

[13] S. Okano, K. Takayama, K. Miura, and A. Morimoto: Study on the Street and Boarding Environment upon the Installation of Level 4 Autonomous Vehicles, *JSTE Journal of Traffic Engineering*, Vol. 6, No. 2, pp. A105—A112 (2020)
[14] J. Wang, Y. Zheng, Q. Xu, J. Wang, and K. Li: Controllability Analysis and Optimal Control of Mixed Traffic Flow with Human-Driven and Autonomous Vehicles, *IEEE Transactions on Intelligent Transportation Systems*, Vol. 22, No. 12, pp. 7445—7459 (2021)
[15] T. Kim and K. Jerath: Congestion-Aware Cooperative Adaptive Cruise Control for Mitigation of Self-Organized Traffic Jams, *IEEE Transactions on Intelligent Transportation Systems*, Early access (2021)
[16] Z. Yao, Y. Wu, Y. Jiang and B. Ran: Modeling the Fundamental Diagram of Mixed Traffic Flow With Dedicated Lanes for Connected Automated Vehicles, '' *IEEE TRANSACTIONS ON INTELLIGENT TRANSPORTATION SYSTEMS* vol. 24, No. 6, pp. 6517—6529 (2023)
[17] A. Schadschneider and M. Schreckenberg: Cellular Automaton Models and Traffic Flow; *Journal of Physics A:Mathematical and Theoretical*, Vol. 26, No. 15, pp. 1–7 (1993)
[18] A. Schadschneider: Modelling of Transport and Traffic Problems: *Cellular Automata. ACRI 2008. Lecture Notes in Computer Science*, Vol. 5191 (2008)
[19] I. Neri, N. Kern, and A. Parmeggiani: Totally Asymmetric Simple Exclusion Process on Networks, Physics Review Letters, Vol. 107, p. 068702 (2011)
[20] T. Imai, and K. Nishinari: Optimal Information Provision for Maximizing Flow in a Forked Lattice, *Physical Review* E, Vol. 91, p. 062818 (2015)
[21] P. Kasture and H. Nishimura: Platoon Definitions and Analysis of Correlation Between Number of Platoons and Jamming in Traffic System, in IEEE Transactions on Intelligent Transportation Systems, Vol. 22, No. 1, pp. 319-328 (2021)
[22] Y. Mochizuki and K. Sawada: An Analysis of Expansion and Reduction Speeds of Traffic Jams on Graph Exploration, *Artificial Life Robotics*, vol. 27, pp. 487–494 (2022)
[23] Y. Mochizuki and K. Sawada: Demand-For Graph Evaluation of Traffic Congestion due to Altruistic Lane Changes of CAVs, *2022 IEEE Conference on Control Technology and Applications (CCTA)*, pp. 334–340 (2022)
[24] B. Priambodo, A. Ahmad, R. A. Kadir: Predicting Traffic Flow Propagation Based on Congestion at Neighbouring Roads Using Hidden Markov Model, " *IEEE Access* vol. 9, pp. 85933 – 8594 (2021)
[25] T. Zhang, J. Xu, S. Cong, C. Qu, and W. Zhao: A Hybrid Method of Traffic Congestion Prediction and Control, " *IEEE Access* vol. 11, pp. 36471 – 36491 (2023)
[26] B.S. Kerner and S.L. Klenov: Phase Transitions in Traffic Flow on Multilane Roads, ' ' *Physical Review E*, Vol. 80, p. 056101 (2010)
[27] D. Helbing and A. Greiner: Modeling and Simulation of Multilane Traffic Flow, " *Physical Review E* Vol. 55, p. 5498 (1997)

YUKARI MOCHIZUKI received her Ph.D. degrees in 2022 from The University of Electro-Communications. Her research interests include the control theory of multi-agent systems. She is a member of SICE.

KENJI SAWADA received his Ph.D. degrees in engineering in 2009 from Osaka University. He is an Associate Professor in Info-Powered Energy System Research Center, The University of Electro-Communications, Japan. He is also an advisor of Control System Security Center since 2016. He received Outstanding Paper Awards from FA Foundation (2015 and 2019), Fluid Power Technology Promotion foundation (2018), and JSME (2018). His research interests include the control theory of cyber-physical systems and control system security. He is a member of SICE, ISCIE, IEEJ, IEICE, JSME, IEEE.